

2020-05-21

Prediction of Shoreline Evolution. Reliability of a General Model for the Mixed Beach Case

Tomasicchio, GR

<http://hdl.handle.net/10026.1/18087>

10.3390/jmse8050361

Journal of Marine Science and Engineering

MDPI

All content in PEARL is protected by copyright law. Author manuscripts are made available in accordance with publisher policies. Please cite only the published version using the details provided on the item record or document. In the absence of an open licence (e.g. Creative Commons), permissions for further reuse of content should be sought from the publisher or author.

Article

Prediction of Shoreline Evolution. Reliability of a General Model for the Mixed Beach Case

Giuseppe R. Tomasicchio ^{1,*} , Antonio Francone ¹, David J. Simmonds ² ,
Felice D'Alessandro ³ and Ferdinando Frega ⁴ 

¹ Engineering Department, University of Salento, 73100 Lecce, Italy; antonio.francone@unisalento.it

² Faculty of Science and Engineering, University of Plymouth, Plymouth PL48AA, UK;
d.simmonds@plymouth.ac.uk

³ Department of Environmental Science and Policy, University of Milan, 20122 Milan, Italy;
felice.dalessandro@unimi.it

⁴ Department of Civil Engineering University of Calabria, 87100 Cosenza, Italy; ferdinando.frega@unical.it

* Correspondence: roberto.tomasicchio@unisalento.it; Tel.: +39-0832-297715

Received: 30 April 2020; Accepted: 19 May 2020; Published: 21 May 2020



Abstract: In the present paper, after a sensitivity analysis, the calibration and verification of a novel morphodynamic model have been conducted based on a high-quality field experiment data base. The morphodynamic model includes a general formula to predict longshore transport and associated coastal morphology over short- and long-term time scales. With respect to the majority of the existing one-line models, which address sandy coastline evolution, the proposed General Shoreline beach model (GSb) is suitable for estimation of shoreline change at a coastal mound made of non-cohesive sediment grains/units as sand, gravel, cobbles, shingle and rock. In order to verify the reliability of the GSb model, a comparison between observed and calculated shorelines in the presence of a temporary groyne deployed at a mixed beach has been performed. The results show that GSb gives a good agreement between observations and predictions, well reproducing the coastal evolution.

Keywords: longshore transport; morphodynamic model; field experiment; mixed beaches

1. Introduction

During the last decades, researchers and engineers inspired by coastal sediment phenomena have conducted field and laboratory experiments to learn more about coastal processes and sediment dynamics. Their efforts have resulted in a wealth of papers and documents published in books, journals, conference and symposium proceedings over the last 50 years [1].

One-line models have shown practical capability in predicting shoreline change, in assisting in the selection of the most appropriate protection design, in the planning of projects located in the nearshore zone [2] and in assessing the longevity of beach nourishing projects. Among the others, the most popular models for shoreline change are Generalized Shoreline Change Numerical Model (GENESIS) [3], ONELINE [4], UNIFORM BEACH SEDIMENT TRANSPORT (UNIBEST) [5], LITTORAL PROCESSES AND COASTLINE KINETICS (LITPACK) [6], BEACHPLAN [7], SISTEMA DE MODELADO COSTERO (SMC) [8], GENESIS and CASCADE (GENCADE) [9]. Each of the aforementioned models is suitable for one type of beach sediments composition solely (e.g., sandy beach or gravel beach) and is subjected to different limitations regarding its use (Table 1). The majority of existing large-scale coastline models address sandy coastline evolution [10]. To date, no general one-line model valid for estimation of shoreline change at a coastal mound made of non-cohesive sediment grains/units as sand, gravel, cobbles, shingle and rock has been proposed.

Table 1. Main features of the existing one-line models.

Model	Variability of Seabed Proprieties	Diffraction Around the Structures	Longshore Current	Longshore Sediment Transport	Groynes	Detached Breakwaters
GENESIS	No	Yes	No	CERC [11]	Yes	Yes
ONELINE	No	Yes	No	Kamphuis [12]	Yes	Yes
UNIBEST	No	No	Yes	Bijker [13] Van Rijn [14] Bailard [15] CERC [11]	Yes	No
LITPACK	Yes	Yes	Yes	STPQ3D [16]	Yes	Yes
BEACHPLAN	Yes	Yes	Yes	CERC [11]	Yes	Yes
SMC	No	Yes	No	CERC [11]	No	No
GENCADE	No	Yes	No	CERC [11]	Yes	Yes

Presently, there is a growing interest in properly defining the morphological processes of gravel, cobbles or shingle/mixed beaches due to an increasing interest for using of coarse sediments in the artificial nourishing of eroded beaches, as they provide a longer longevity of the nourishing intervention under the forcing processes during storm events [17–19]. In this context, one has to consider that the use of models in practical design situations could also be linked to economic and financial considerations when a cost–benefit approach is part of the design; conversely, models can help in examining the economic implications of a design [20]. Moreover, when designing a coastal protection intervention, modern Coastal Engineering extensive use of numerical models to predict impact of the designed intervention before it is implemented.

Within this path, the focus of the present paper is to propose a novel model, named the General Shoreline beach model (GSb), for predicting shoreline change for beaches made of non-cohesive sediment grains/units and to show the results of a sensitivity analysis conducted to evaluate how model output changes with changes in input variables [21,22]; the sensitivity analysis allows to assess the effects and sources of uncertainties oriented to the target to build a robust model for shoreline evolution. The calibration and verification of the GSb model for predicting shoreline change at a mixed beach are performed based on a high-quality field experiment data base [23–25].

2. Materials and Methods

2.1. The General Longshore Transport Model (GLT)

Longshore transport due to oblique waves acting on beaches made of non-cohesive sediment grains/units as sand, gravel, cobbles, shingle and rock is determined by means of the General Longshore Transport (GLT) model [26–28]. The GLT model belongs to the typology based on an energy flux approach combined with an empirical relationship between the wave induced forcing and the number of moving sediment grains/units. Specifically, the GLT model considers an appropriate mobility index and assumes that the units move during up- and down-rush with the same obliquity of breaking and reflected waves at the breaker depth [26]. A sediment grain/unit passes through a certain control section if and only if it is removed from an updrift area of extension equal to the longitudinal component of the displacement length, $l_d \sin\theta_d$, where l_d is the displacement length and θ_d is its obliquity (Figure 1).

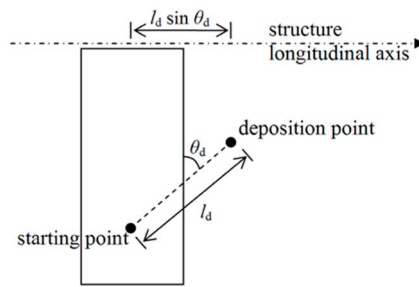


Figure 1. Definition sketch for the General Longshore Transport (GLT) model.

This process description is particularly true when considering the wave obliquity, the up-rush and related longshore transport at the swash zone. By assuming that the displacement obliquity is equal to the characteristic wave obliquity at breaking ($\theta_d = \theta_{k,b}$), and that a number N_{od} of particles removed from a nominal diameter, D_{n50} , wide strip moves under the action of 1000 waves, then the number of units passing a given control section in one wave is:

$$S_N = \frac{l_d}{D_{n50}} \cdot \frac{N_{od}}{1000} \sin\theta_{k,b} = f(N_s^{**}), \tag{1}$$

where:

$$N_s^{**} = \frac{H_k}{C_k D_{n50}} \left(\frac{s_{m,0}}{s_{m,k}} \right)^{-1/5} (\cos\theta_0)^{2/5}. \tag{2}$$

N_s^{**} is the modified stability number [26] with: H_k = characteristic wave height; $C_k = H_k/H_{s,0}$, where $H_{s,0}$ = significant offshore wave height; θ_0 = offshore wave obliquity; $s_{m,0}$ = mean wave steepness at offshore conditions and $s_{m,k}$ = characteristic mean wave steepness (assumed equal to 0.03). N_s^{**} resembles the traditional stability number, N_s [29,30], taking into account the effects of a non-Rayleighian wave height distribution at shallow water [31], wave steepness, wave obliquity and the nominal diameter of the sediment grains/units. The authors in [26,32] reported that H_k is to be considered equal to $H_{1/50}$, but $H_{2\%}$ can also be adopted. In the first case $C_k = 1.55$, in the second case $C_k = 1.40$. The second factor in Equation (2) is such that $N_s^{**} \cong N_s$ for $\theta_0 = 0$ if $s_{m,0} = s_{m,k}$.

In the case of a head-on wave attack, under the assumption that, offshore the breaking point, the wave energy dissipation is negligible and that waves break as shallow water waves, the following relation holds:

$$F = 1/8 \rho g H_0^2 c_{g,0}^2 = 1/8 \rho g H_b^2 c_{g,b}^2, \tag{3}$$

In Equation (3), F = wave energy flux, ρ = water density, g = gravity acceleration, H_0 = offshore wave height, $c_{g,0}$ = offshore wave group celerity, H_b = wave height at breaking and $c_{g,b}$ is the wave group celerity at breaking.

Equation (3), related to the breaker index $\gamma_b = H_b/h_b$, with h_b = breaking depth, implies:

$$H_b = H_0 \left(\frac{\gamma_b}{4k_0 H_0} \right)^{1/5} = q H_0 s_0^{-1/5}, \tag{4}$$

The authors in [33] found the best agreement with field and laboratory data assuming $\gamma_b = 1.42$ or the proportionality constant $q = 0.56$. It follows that, considering the characteristic wave height at breaking, $H_{k,b}$, and $s_{m,0} = s_{m,k} = 0.03$, N_s^{**} can be also written as:

$$N_s^{**} \cong \frac{0.89 H_{k,b}}{C_k D_{n50}}, \tag{5}$$

where Δ = relative mass density of the sediment grain/unit = $(\rho_s - \rho)/\rho$ and ρ_s = sediment grain/unit density.

According to the refraction theory for plane and monotonically decreasing profiles, $H_{k,b}$ and $\sin\theta_{k,b}$, are evaluated as in the following [26,34]:

$$H_{k,b} = \left(H_k^2 c_g \cos \theta_o \sqrt{\gamma_b / g} \right)^{2/5}, \tag{6}$$

$$\sin \theta_{k,b} = \frac{c_{k,b}}{c} \sin \theta_o, \tag{7}$$

$$c_{k,b} = \sqrt{g H_{k,b} / \gamma_b}, \tag{8}$$

where c_g = group celerity and $c_{k,b}$ is the characteristic wave celerity at breaking depth.

The displacement length is calculated as [26]:

$$l_d = \frac{(1.4N_s^{**} - 1.3)}{\tanh^2(kh)} D_{n50}, \tag{9}$$

where k = wave number and h = water depth.

N_{od} has been determined following a calibration procedure based on the least-squares method, taking into account nine high quality data sets of longshore transport from field and laboratory experiments for a wide mobility range of sediment grains/units: from stones to sand. In total, the nine data sets consist of 245 cases [28]. In particular, N_{od} values are partitioned in two intervals: the first interval refers to $N_s^{**} \leq 23$, from reshaping type berm breakwaters [35] to gravel beaches; the second one relates to $N_s^{**} > 23$, for sandy beaches. For $N_s^{**} \leq 23$, a third order polynomial approximating function provides a satisfactory agreement as shown by [28]. For $N_s^{**} > 23$ a good agreement is obtained by a linear regression in log–log plane. N_{od} is given as:

$$N_{od} = \begin{cases} 20N_s^{**}(N_s^{**} - 2)^2 & N_s^{**} \leq 23 \\ \exp[2.72 \ln(N_s^{**}) + 1.12] & N_s^{**} > 23 \end{cases}, \tag{10}$$

The estimated correlation coefficient is equal to 0.89 for $N_s^{**} \leq 23$ and 0.92 for $N_s^{**} > 23$.

The longshore transport rate, Q_{LT} , can be also expressed in terms of [m³/s] as in the following:

$$Q_{LT} = \frac{S_N D_{n50}^3}{(1 - n) T_m}, \tag{11}$$

where T_m = mean wave period, and n = porosity factor.

Figure 2 shows the flowchart summarizing the use of the GLT.

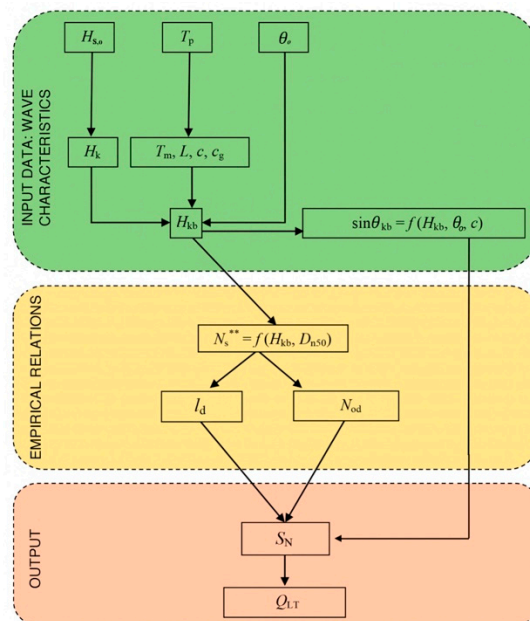


Figure 2. User flowchart.

2.2. The General Shoreline Beach Model (GSb)

2.2.1. Theoretical Background

The GSb model belongs to the one-line model typology [36] and assumes that the beach cross-shore profile remains unchanged [37,38], thereby allowing beach change to be described uniquely in terms of the shoreline position.

The equilibrium cross-shore profile is calculated as proposed by [37,38] and is used to determine the average nearshore bottom slope adopted in longshore transport equation. The average cross-shore profile is described by [37]:

$$h(y) = Ay^{2/3}, \quad (12)$$

where h is expressed in (m), A = scale parameter ($m^{1/3}$) and y = offshore distance from the initial shoreline (m). The scale parameter A can be calculated as in the following [39]:

$$A = 0.41(D_{n50})^{0.94}, \quad D_{n50} < 0.4 \text{ mm}, \quad (13)$$

$$A = 0.23(D_{n50})^{0.32}, \quad 0.4 \text{ mm} \leq D_{n50} < 10.0 \text{ mm}, \quad (14)$$

$$A = 0.23(D_{n50})^{0.28}, \quad 10.0 \text{ mm} \leq D_{n50} < 40.0 \text{ mm}, \quad (15)$$

$$A = 0.46(D_{n50})^{0.11}, \quad D_{n50} \geq 40 \text{ mm}, \quad (16)$$

The main peculiarity of the GSb model is the use of the GLT model, allowing to have an explicit dependence of shoreline evolution on D_{n50} [28,40]. This finding is due to the fact that GSb uses the GLT model. Differently from GENESIS and similar models [7,8,41], which take into account two calibration coefficients, K_1 and K_2 , the GSb presents one calibration coefficient, K_{GSb} , which does not solely depend on the grain size diameter and depends on the longshore gradient in breaking wave height [42].

As in the case of most numerical models (e.g., GENCADE [9]), GSb is able to deal with the presence of soft and hard coastal structures. Soft protection consists of nourishing an eroded beach. A hard intervention consists in deployment of one or more coastal structures (e.g., groynes, detached breakwaters and seawalls), composed by natural rock or artificial concrete units.

The model allows to determine short-term (daily base) or long-term (yearly base) shoreline change [43,44] for arbitrary combinations and configurations of hard structures and beach fills that can be represented on a modelled reach of coast.

GSb considers the sediment grain/unit passing around or through a coastal structure. Two types of sediment movement around or through the structures can be simulated: bypass, when the sediment passes around the seaward end of the groynes, and transmission, where the sediment passes through the structures. Specifically, bypass occurs when the water depth at the tip of the structure, D_G , is less than the depth of active longshore transport, D_{LT} , calculated with [45]. To represent sediment bypass, a bypassing factor, BF , is defined as:

$$BF = 1 - \frac{D_G}{D_{LT}} \quad D_G \leq D_{LT}, \quad (17)$$

Transmission occurs due to permeability of the material, p , composing the coastal structure. With $p = 0$, the structure is completely transparent. On the contrary, for $p = 1$, the structure is fully impermeable. With the values of BF and p , GSb calculates the total fraction TF of sediment passing around or through a structure as defined by [41]:

$$TF = p(1 - BF) + BF, \quad (18)$$

The TF value is calculated at every time step for each structure present in the model domain.

GSb takes into account the wave transformation phenomena as shoaling, refraction and diffraction. Shoaling and refraction are treated according to an internal wave model proposed by [39]. GSb uses

the simplified diffraction calculation procedure from waves with directional spread presented by [46] to represent diffraction at structures such as detached breakwaters and groynes.

The model requires predictive expressions for the longshore sediment transport rate.

2.2.2. Longshore Sediment Transport Rate

The GSb model uses the following equation for the longshore transport rate Q_l :

$$Q_l = \frac{S_N D_{n50}^3}{(1-n)T_m} - \frac{K_{GSb}}{8\left(\frac{\rho_s}{\rho} - 1\right)(1-n)\tan\beta} H_{s,b}^2 c_{g,b} \cos(\theta_{bs}) \frac{\partial H_{s,b}}{\partial x}, \quad (19)$$

where $\tan\beta$ = average bottom slope from the shoreline to the closure depth, d_c ; $H_{s,b}$ = significant wave height at breaking; θ_{bs} = angle of breaking waves to the local shoreline; x = longshore distance.

The first term in Equation (19) accounts for longshore transport as from the ‘‘GLT formula’’ [26,27]. The second term in Equation (19), similar to GENESIS [39], ONELINE [4], BEACHPLAN [7], SMC [8] and GENCADE [9], accounts for the longshore sediment transport induced by the longshore gradient in significant wave height at breaking [42], where $H_{s,b}$ is calculated taking into account the wave propagation shoaling, refraction and diffraction phenomena [39]. The original formulation of the second term in Equation (19) considers the root-mean-square (rms) wave height [42]. The factor 1.416 is used to convert from significant wave height to root-mean-square (rms) wave height [39].

2.2.3. Sediment Continuity Equation

Spatial and temporal variations in gradients in longshore transport drive shoreline accretion/erosion. The relation between shoreline evolution in terms of accretion/erosion, Δy , and the longshore transport rate is formulated considering the continuity equation of sediment in a control volume, V (Figure 3).

The sediment continuity equation expressed as:

$$\frac{\Delta V}{\Delta t}(1-n)(d_b + d_c) + \frac{Q_l}{x} = 0, \quad (20)$$

where d_b = berm height and t = time, is solved by an explicit finite difference scheme [39].

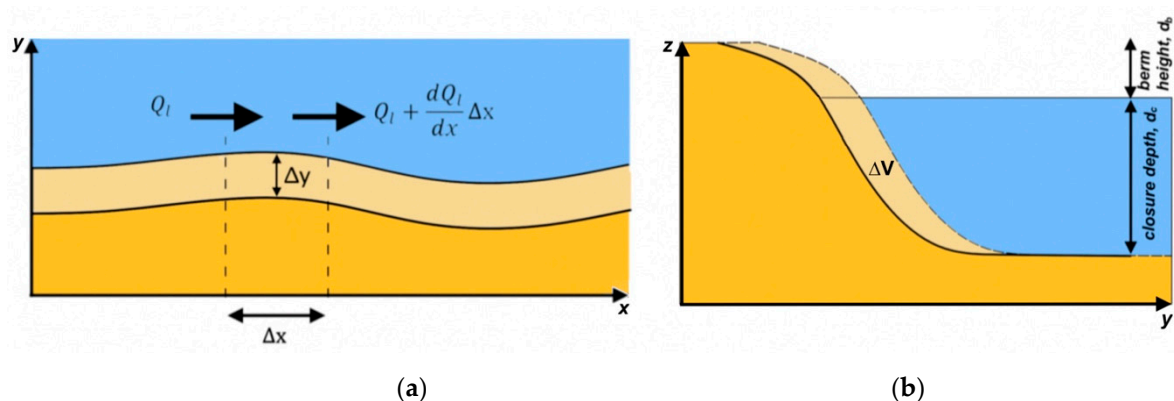


Figure 3. (a) Longshore sediment transport rate Q_l and coastal evolution Δy ; (b) beach cross-shore profile change.

2.3. Influence of Different Inputs

Models are sensitive to morphological as well as forcing input parameters; thus, it is imperative to use proper values and to perform a sensitivity analysis to evaluate how model output changes with changes in input parameters [21,22]; if a small modification in a parameter value produces a large change in the output, model reliability is low and vice versa [47].

In the present paper, in order to evaluate the reliability of the GSb model, a sensitivity analysis for a range of selected input parameters has been conducted based on the simulation of the advance/retreat of an initial straight shoreline in presence of a single groyne. Specifically, three input parameters have been selected as representative of (i) wave characteristics (i.e., ϑ_o), (ii) sediment properties (i.e., D_{n50}) and (iii) short/long term predictions (i.e., duration of simulation, t).

Simulations have been performed for the same conditions considered by [9] and shown in Table 2; this has allowed a direct comparison with the results to be obtained by using GENCADE [9] (Figure 4). As an initial condition, a straight shoreline 3000 m long with a 75 m long single groyne located at the center of the domain has been considered. The cross-shore beach profile, with $D_{n50} = 0.3$ mm, is characterized by a berm height of 1 m with a closure depth equal to 8 m. With regard to the input offshore wave characteristics, values of $H_{s,o} = 0.75$ m, and $T_p = 8$ s at 50 m water depth have been simulated. The model grid cell resolution, DX , has been assumed equal to 10 m with a total number of cells, $NX = 300$. A calculation time step, DT , equal to 0.5 h has been adopted. For $t = 2$ years, GSb has been run with $K_{GSb} = K_2 = 0.25$; the boundary condition has been set as *fixed*. *Fixed* means that the boundary will not move from the initial shoreline over the calculation interval (i.e., y does not change over time).

Table 2. Selected input parameters.

D_{n50} (mm)	0.3
D_B (m)	1
D_C (m)	8
$H_{s,o}$ (m)	0.75
T_p (s)	8
ϑ_o (deg)	15
DX (m)	10
NX (-)	300
DT (h)	0.5
t (years)	2
K_{GSb} (-)	0.25

Figure 4 shows that, for both models, the shoreline results in agreement with the expected up-drift deposition and down-drift erosion phenomena. However, no judgment can be given on their reliability in absence of field data.

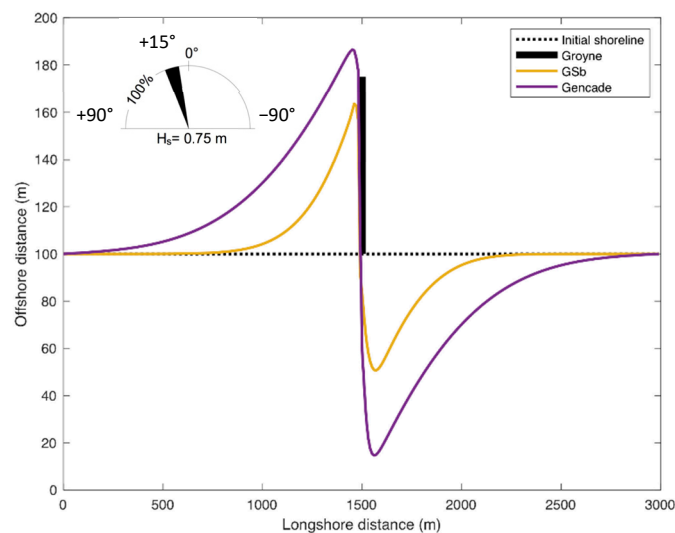


Figure 4. Comparison between GSb and GENCADE.

2.3.1. Influence of Offshore Wave Angle

In order to evaluate the influence of the offshore wave angle on the shoreline evolution, different values of ϑ_0 in the interval from -45 to $+45$ deg have been considered. The adopted input parameters are given in Table 2, with $\vartheta_0 = -45, -35, -15, -5, +5, +15, +25, +35, +45$ deg.

Figure 5 shows the calculated shoreline evolution induced by longshore transport acting from (a) right to left for $\vartheta_0 = -45, -35, -25, -15, -5$ deg, and (b) from left to right for $\vartheta_0 = +5, +15, +25, +35, +45$ deg, respectively.

Maximum and minimum advance/retreat rates have been obtained for $\vartheta_0 = \pm 35$ and $\vartheta_0 = \pm 5$, respectively.

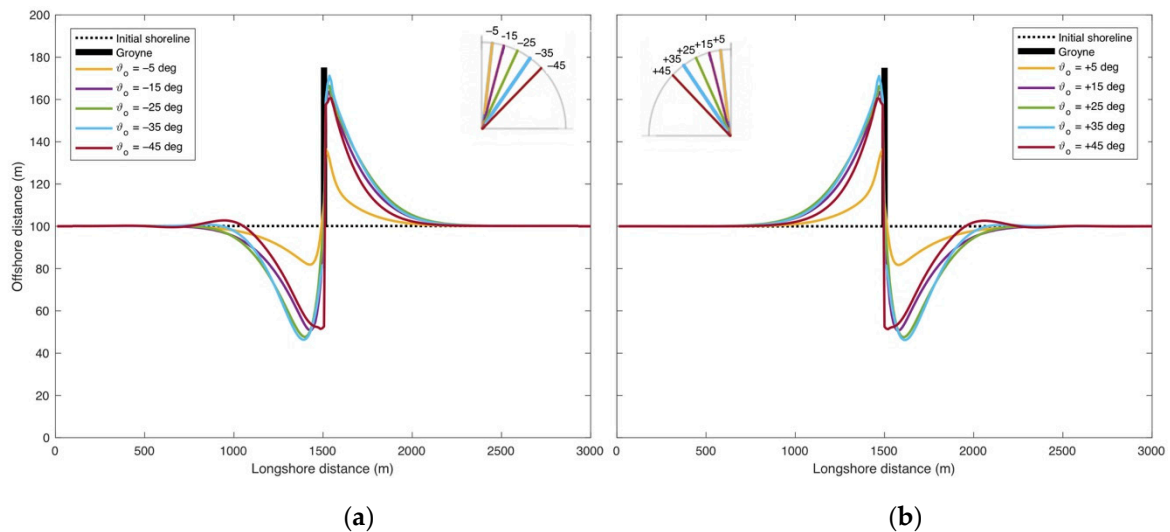


Figure 5. Calculated shoreline evolution for (a) $\vartheta_0 = -45, -35, -15, -5$ and (b) $\vartheta_0 = +5, +15, +25, +35, +45$.

2.3.2. Influence of Nominal Diameter

In order to evaluate the influence of the nominal diameter on the shoreline evolution, different values of D_{n50} have been considered. The adopted input parameters are given in Table 2, with $D_{n50} = 0.3, 30$ and 100 mm corresponding to sand, pebbles and cobbles, respectively.

Figure 6 shows the calculated shoreline evolution induced by longshore transport.

A lower mobility of the sediment grain/unit composing the beach is found when considering a larger sediment diameter. On the left (updrift)/right (downdrift) side of the groyne, shoreline advance/retreat rates, equal to 60, 40 and 20 m, have been obtained for $D_{n50} = 0.3, 30$ and 100 mm, respectively.

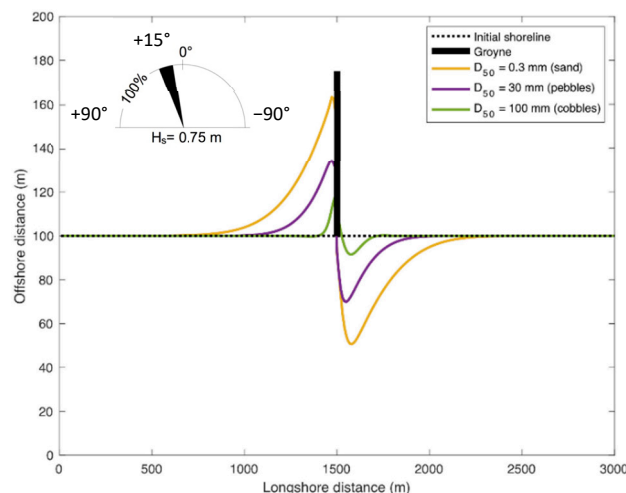


Figure 6. Calculated shoreline evolution for $D_{n50} = 0.3$ mm, 30 mm, 100 mm.

2.3.3. Influence of Duration

In order to assess the capacity of the model to determine short-term (daily base), medium-term (monthly base) or long-term (yearly base) shoreline evolution, different values of duration of simulation have been considered. The adopted input parameters are given in Table 2, with $t = 1$ day, 1 month, 6 months, 1 year, 2 years. Figure 7 shows the calculated shoreline evolution induced by longshore transport.

The shoreline advance/retreat rate increases with a longer duration of simulation. On the left (updrift)/right (downdrift) side of the groyne, shoreline advance/retreat rates, equal to 2.1, 14.2, 40.9, 52.4 and 63.6 m, have been obtained for $t = 1$ day, 1 month, 6 months, 1 year and 2 years, respectively.

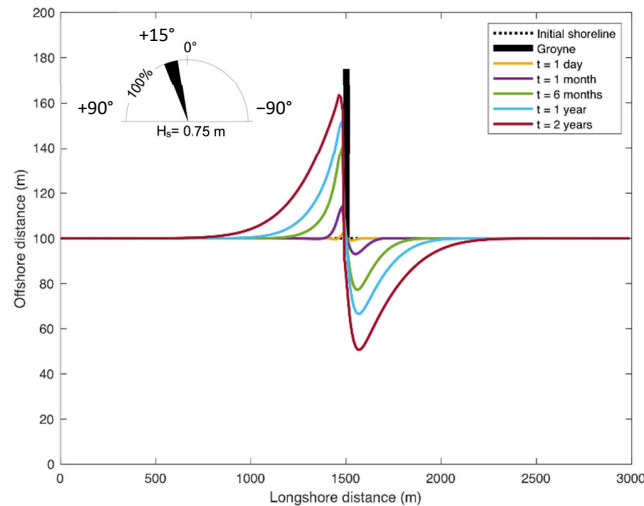


Figure 7. Calculated shoreline evolution for $t = 1$ day, 1 month, 6 months, 1 year, 2 years.

2.4. Field Experiment at a Mixed Beach

Study Area and Field Observations

Shoreline evolution has been observed during a field experiment conducted in 2007 at Milford-on-Sea, under Hordle Cliff, located in the county of Hampshire on the Southern coast of the UK [23–25]. The coastal area of Milford-on-Sea, at the eastern side of Christchurch Bay (Figure 8), is characterized by a mixed shingle and sand beach, composed by finer (sand) and coarse (cobbles, gravel) sediment units/grains ($D_{n50} = 11.19$ mm; $D_{85}/D_{15} = 27.79$, where D_{85} and D_{15} represent the particle diameter for which 85% and 15%, respectively, of the material is finer) (Figure 9).

An impoundment technique has been adopted consisting of a temporary impermeable groyne 46 m long (originally 19 m wet and 27 dry) deployed along the beach for the period 1 October 2007–15 November 2007, acting as a barrier for the sediments moving along the coast (Figure 10a). This technique is considered by several authors as a reliable and effective method to estimate longshore transport rates [40,48–50].



Figure 8. Study area location.

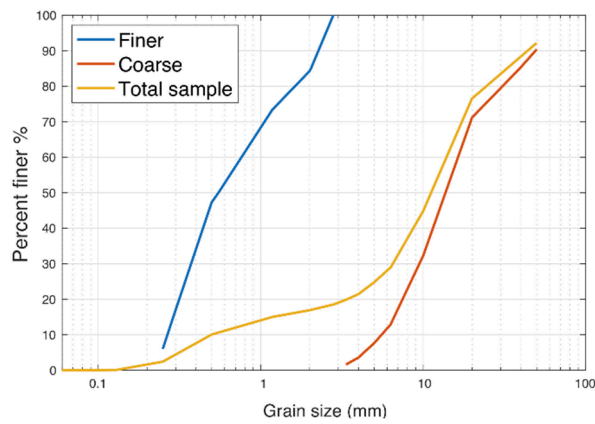


Figure 9. Sediment unit/grain size distribution curves.



Figure 10. (a) View of the temporary structure from the top of Hordle Cliff the 6 October 2007; (b) plan view of the study site and groyne position.

A Differential Global Positioning System (DGPS) has been used to perform the beach profile surveys at low tide condition, covering an extension of 280 m alongshore (Figure 10b) [23]. Wave data have been collected by an Acoustic Wave and Current (AWAC) profiler from 1 October 2007 to 25 November 2007 (Figures 11 and 12); data have been recorded in intervals of one hour, approximately 600 m at 7 m water depth.

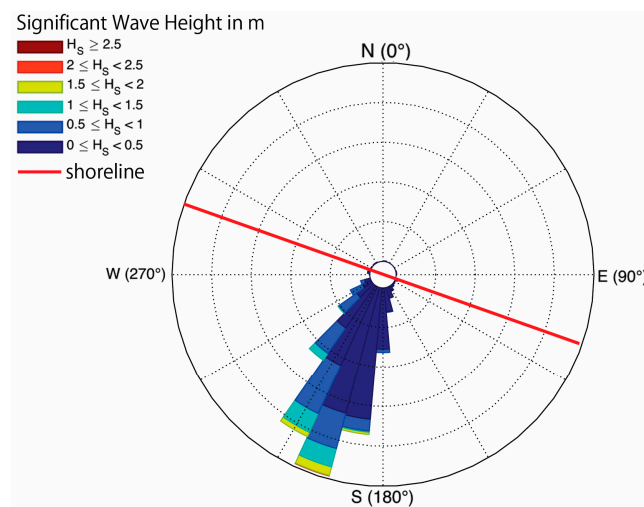


Figure 11. Wave rose and shoreline orientation.

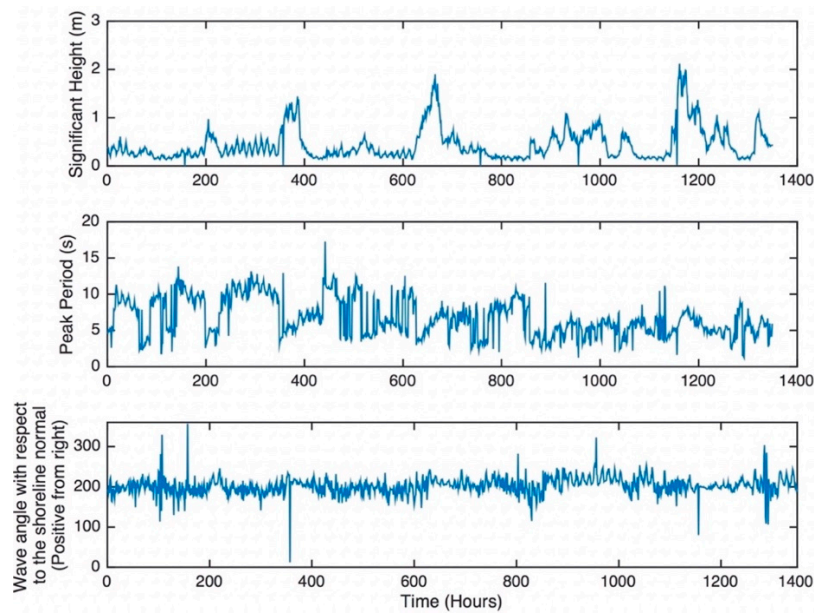


Figure 12. Time history of significant wave height, peak period and wave angle.

3. GSb Calibration and Verification for a Mixed Beach

3.1. Calibration

The calibration of the GSb model has been conducted based on the comparison between the observed and calculated shoreline evolution. Values of $K_{GSb} = 0.005, 0.01, 0.05, 0.1, 0.2$ have been adopted. The first beach survey collected in presence of the groyne (1 October 2007) has been assumed as the initial shoreline. Based on an accurate evaluation of the cross-shore beach profile evolution over time, D_C and D_B have been selected equal to 1 m and 3 m, respectively (Figure 13) [23]. A value of $D_{n50} = 11.19$ mm has been adopted. The considered groyne has been positioned at the 31st cell of the domain, corresponding to $x = 150/155$ m. Hourly wave conditions (H_s, T_p, Dir) have been considered in the simulations (Figures 11 and 12). The computational domain has been assumed 280 m long; DX has been set equal to 5 m with $NX = 57$. The calculation time step has been set to 0.05 h (180 s), for a total duration of simulation equal to 45 days from the groyne deployment ($t = 0$). In accordance with [11] the boundary conditions have been set as *fixed*, since they are located far away from the groyne (i.e., the length of the entire calculation domain is in the order of two or three groyne length). It assures that the boundary conditions are unaffected by changes that take place in the vicinity of the groyne.

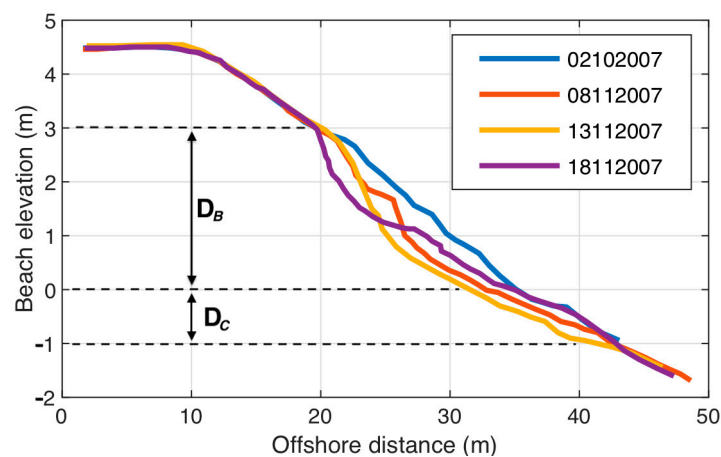


Figure 13. Surveied cross-shore beach profile at Milford-on-Sea.

Figure 14 shows for the selected values of K_{GSb} , (i) the comparison between observed and calculated shorelines at the end of the simulation (45 days) and (ii) the corresponding values of Root Mean Square Error ($RMSE$). The value of $K_{GSb} = 0.1$ gave the better agreement between observed and calculated shoreline showing the lowest ($RMSE$) value, equal to 4.6. The difference among all the estimated $RMSE$ values is lower than 0.2. K_{GSb} depends on the longshore gradient in breaking wave height. For the considered field case, a single groyne deployed on a smooth uniform bathymetry, the longshore gradient in breaking wave height is moderate. Consequently, the results were less sensitive to the value of K_{GSb} . It was noticed that the observed shoreline moves at the boundary and the sediment mass seems to be not conserved.

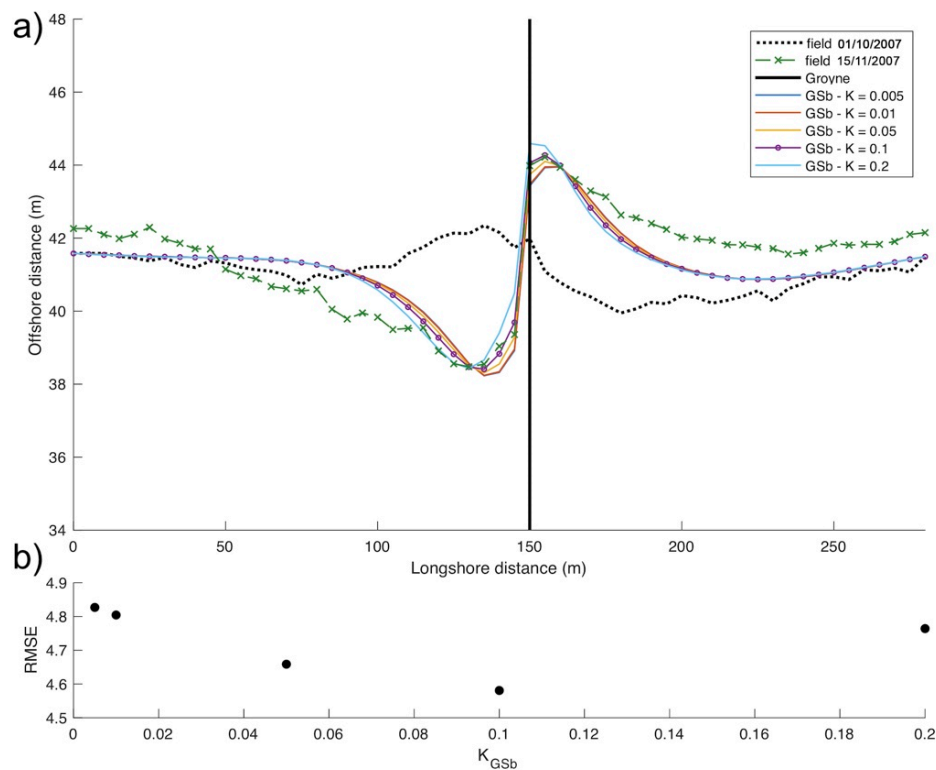


Figure 14. (a) Observed and calculated shorelines at the end of the simulation (45 days) for the selected values of K_{GSb} (b) $RMSE$ vs. K_{GSb} .

3.2. Verification

Calibration of GSb has been obtained by comparing the calculated and observed shorelines after 45 days; a value of $K_{GSb} = 0.1$ has been assumed. It is of a certain interest to verify the reliability of GSb at daily steps within the 45 days. $RMSE$ daily values are shown in Figure 15a, with maximum values attained at the two storms occurred on 16th and 27th days after the groyne deployment. This behavior is probably due to the deviation of the beach cross-shore profile under a severe storm attack from the equilibrium cross-shore profile assumed for a one-line model.

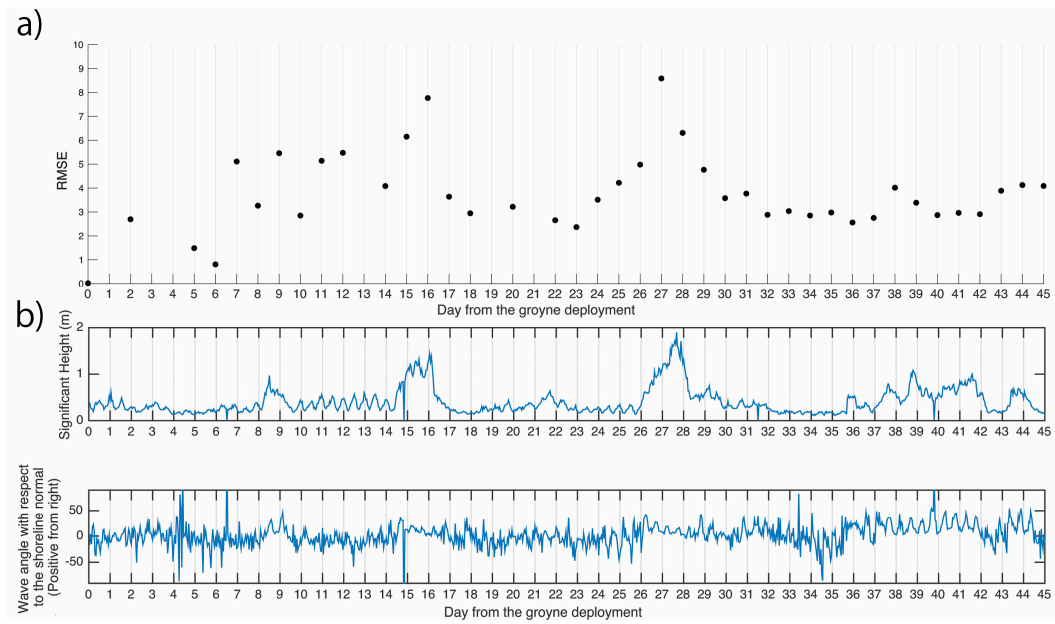


Figure 15. (a) Estimated RMSE daily values. (b) Time history of significant wave height and wave angle.

Figures 16–18 show, as representative cases, the comparison between observed and calculated shorelines, and the difference, $Y_{obs} - Y_{GSb}$, after 24 days (25 October 2007), 39 days (09 November 2007) and 45 days (15 November 2007) from the groyne deployment. Y_{obs} and Y_{GSb} are the distances from the x-axis to the observed and calculated shorelines, respectively.

The comparisons show a good agreement between observed and calculated shorelines at both groyne sides. In particular, after 24 days (Figure 16) from the groyne deployment, a shoreline advance on the left side of the groyne has been observed; after 39 days (Figure 17) and 45 days (Figure 18) from the groyne deployment, a shoreline advance on the right side of the groyne has been observed. GSb calculated the up-drift side changes occurred during the entire period of the simulation.

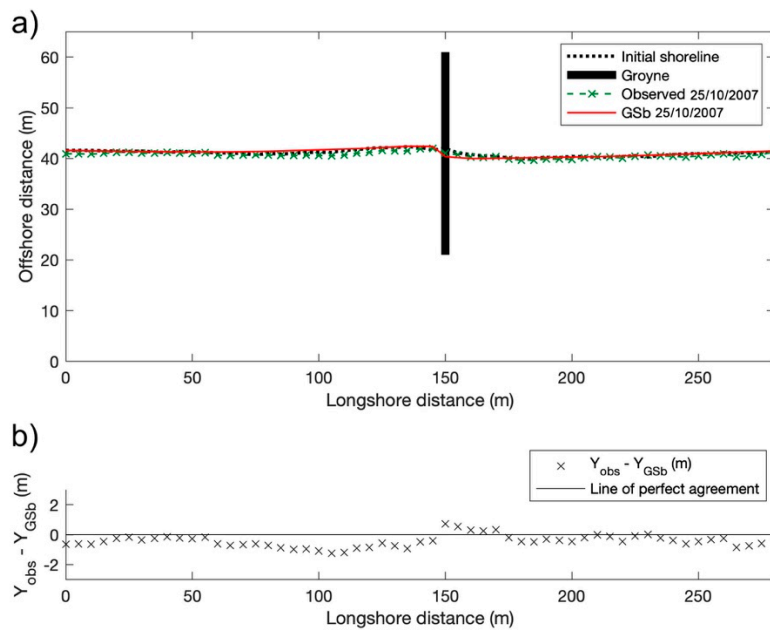


Figure 16. (a) Observed and calculated shorelines after 24 days from the groyne deployment. (b) Difference $Y_{obs} - Y_{GSb}$.

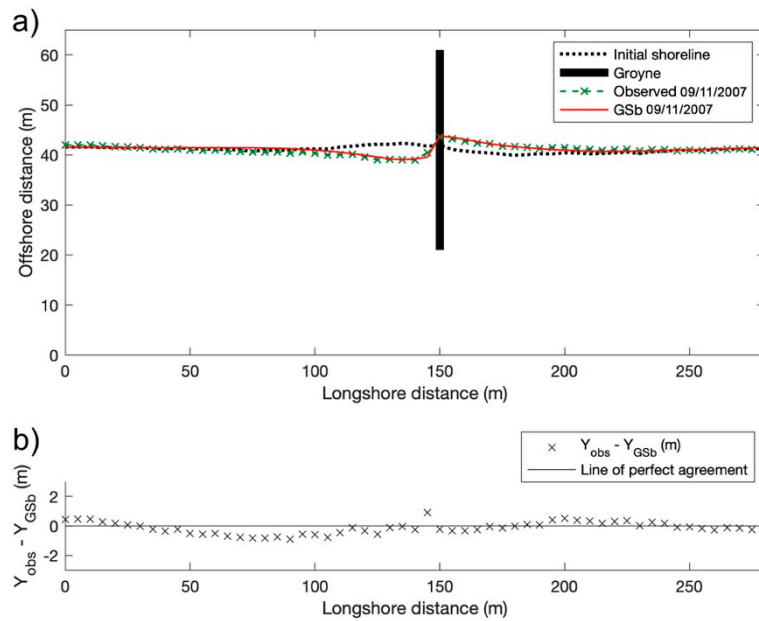


Figure 17. (a) Observed and calculated shorelines after 39 days from the groyne deployment. (b) Difference $Y_{obs} - Y_{GSb}$.

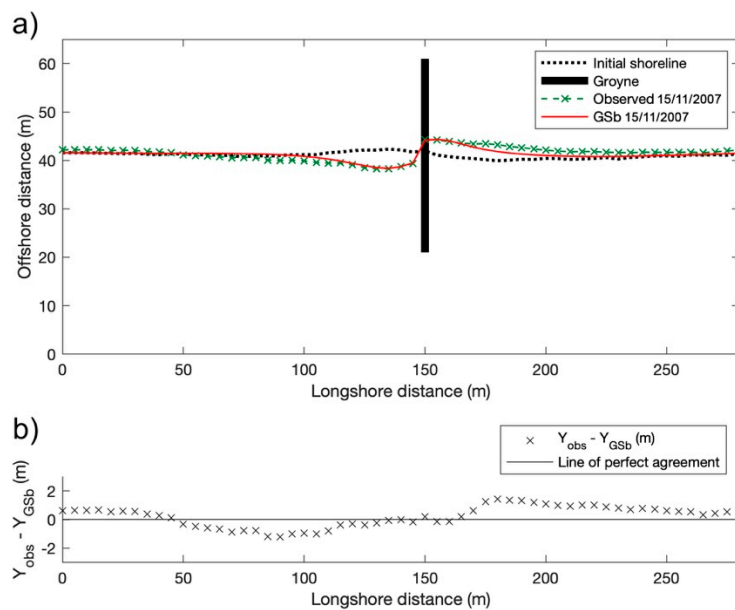


Figure 18. (a) Observed and calculated shorelines after 45 days from the groyne deployment. (b) Difference $Y_{obs} - Y_{GSb}$.

4. Conclusions

To date, the development and use of morphodynamic models focusing on sandy beaches have received the bulk of the attention. Belonging to the one-line model typology, the GSb model is proposed including a general formula suitable for estimation of longshore transport at coastal mound made of non-cohesive sediment grains/units as sand, gravel, cobbles, shingle and rock.

As its main peculiarity, GSb allows to have an explicit dependence of shoreline evolution on D_{n50} . This finding is due to the fact that GSb uses the GLT model. Differently from GENESIS and similar models, which take into account two calibration coefficient, K_1 and K_2 , the GSb model presents one calibration coefficient, K_{GSb} , which does not depend on the grain size diameter and depends on the longshore gradient in breaking wave height, solely.

The reliability of the GSb model to predict coastal morphology over short- and medium-term time scales has been verified based on a high-quality field experiment data base from a specific field case at a mixed beach. Such a source of data is rarely available; indeed, most published sources of shingle/mixed beach data failed on the lack of concurrent wave measurements and transport rates. As a result, the comparison between observed and calculated shorelines in the presence of a temporary groyne shows the premonitory signs that the GSb model can represent a reliable engineering tool suitable for predicting coastal evolution at a mixed beach.

A demo version of the numerical model can be downloaded by following the instructions in the supplementary material section.

Supplementary Materials: A demo version of the GSb numerical model, for Mac and Windows systems, has been made available for the scientific community and can be downloaded at: www.scacr.eu, www.eumer.eu.

Author Contributions: Conceptualization, G.R.T., F.F. and A.F.; methodology, G.R.T., D.J.S., F.D. and A.F.; software, A.F., G.R.T. and F.F.; validation, G.R.T., F.F. and A.F.; formal analysis, G.R.T., F.D. and A.F.; investigation, G.R.T., D.J.S., F.D., F.F. and A.F.; data curation, D.J.S.; supervision, G.R.T.; funding, G.R.T. and D.J.S. All authors have read and agreed to the published version of the manuscript.

Funding: The present work has been supported by the Regione Puglia through the grant to the budget of the project titled “Sperimentazione di tecnologie innovative per il consolidamento di dune costiere (INNO-DUNECOST),” POR Puglia FESR FSE 2014–2020-Sub-Azione 1.4.B, Contract n. RM5UKM3. The field experiment of the present research was funded by the Faculty of Technology of Plymouth University and the EPSRC (Engineering and Physical Sciences Research Council) under the Grant EP/C005392/1 “A Risk-based Framework for Predicting Long-term Beach Evolution”. The work has been also supported by Regione Calabria, through the PhD grant for international exchange.

Acknowledgments: We gratefully acknowledge the University of Salento, Department of Engineering, the University of Calabria, Department of Civil Engineering, and University of Plymouth, COAST Engineering Research Group, which permitted the international exchange making possible this research. We thank Mark Davidson of CPRG at Plymouth University for his contribution relating to field data. We gratefully acknowledge the comments of the three anonymous reviewers who helped to substantially improve the original version of this manuscript.

Conflicts of Interest: The authors declare no conflict of interest.

References

1. Van Rijn, L.C.; Ribberink, J.S.; Werf, J.V.D.; Walstra, D.J. Coastal sediment dynamics: Recent advances and future research needs. *J. Hydraul. Res.* **2013**, *51*, 475–493. [[CrossRef](#)]
2. Güner, H.A.A.; Yüksel, Y.; Çevik, E.Ö. Determination of Longshore Sediment Transport and Modelling of Shoreline Change. *Sediment Transp.* **2011**, *117*. [[CrossRef](#)]
3. Hanson, H. GENESIS: A generalized shoreline change numerical model. *J. Coast. Res.* **1989**, *5*, 1–27.
4. Dabees, M.; Kamphuis, J.W. ONELINE, a numerical model for shoreline change. In Proceedings of the 26th Int. Conf. On Coastal Engineering, ASCE, Copenhagen, Denmark, 22–26 June 1998; pp. 2668–2681.
5. Deltares. *UNIBEST-CL+ Manual: Manual for Version 7.1 of the Shoreline Model UNIBEST-CL.*; Deltares: Delft, The Netherlands, 2011.
6. DHI. *Litpack: Noncohesive Sediment Transport in Currents and Waves. User Guide*; Danish Hydraulic Institute: Hørsholm, Denmark, 2005.
7. Blanco, B. *Beachplan (Version 04.01) Model. Description*; HR Wallingford Report; Springer Nature: Berlin/Heidelberg, Germany, 2003.
8. González, M.; Medina, R.; González-Ondina, J.; Osorio, A.; Méndez, F.; García, E. An integrated coastal modeling system for analyzing beach processes and beach restoration projects, SMC. *Comput. Geosci.* **2007**, *33*, 916–931. [[CrossRef](#)]
9. Frey, A.E.; Connell, K.J.; Hanson, H.; Larson, M.; Thomas, R.C.; Munger, S.; Zundel, A. *GenCade Version 1 Model. Theory and User's Guide*; Engineer Research And Development Center, Vicksburg Ms Coastal Inlets Research Program: Vicksburg, MS, USA, 2012.
10. Vionnet, C.; García, M.H.; Latrubesse, E.; Perillo, G. *River, Coastal and Estuarine Morphodynamics*; RCEM 2009, Two Volume Set; CRC Press: Boca Raton, FL, USA, 2018.

11. USACE. *Shore Protection Manual*; Dept. of the Army, Waterways Experiment Station, Corps of Engineers; Coastal Engineering Research Center: Vicksburg, MS, USA, 1984.
12. Kamphuis, J.W. Alongshore sediment transport rate. *J. Waterw. Port Coast. Ocean Eng.* **1991**, *117*, 624–640. [[CrossRef](#)]
13. Bijker, E.W. Longshore transport computations. *J. Waterw. Harb. Coast. Eng. Div.* **1971**, *97*, 687–701.
14. Van Rijn, L.C. *Principles of Sediment Transport In Rivers, Estuaries And Coastal Seas*; Aqua Publications: Amsterdam, The Netherlands, 1993; Volume 1006.
15. Bailard, J.A. An energetics total load sediment transport model for a plane sloping beach. *J. Geophys. Res. Ocean* **1981**, *86*, 10938–10954. [[CrossRef](#)]
16. DHI. *Littoral Processes FM, User Guide*; Danish Hydraulic Institute: Hørsholm, Denmark, 2017.
17. Tomasicchio, G.R.; D'Alessandro, F.; Musci, F. A multi-layer capping of a coastal area contaminated with materials dangerous to health. *Chem. Ecol.* **2010**, *26*, 155–168. [[CrossRef](#)]
18. Bramato, S.; Ortega-Sánchez, M.; Mans, C.; Losada, M.A. Natural Recovery of a Mixed Sand and Gravel Beach after a Sequence of a Short Duration Storm and Moderate Sea States. *J. Coast. Res.* **2012**, *28*, 89–101. [[CrossRef](#)]
19. Van Rijn, L.C. A simple general expression for longshore transport of sand, gravel and shingle. *Coast. Eng.* **2014**, *90*, 23–39. [[CrossRef](#)]
20. Hanson, H.; Kraus, N.C. Optimization of beach fill transitions. In Proceedings of the Coastal Zone, ASCE, New York, NY, USA, 19–23 July 1993; pp. 103–117.
21. Van Alphen, J.S.; Hallie, F.P.; Ribberink, J.S.; Roelvink, J.; Lousse, C.J. Offshore sand extraction and nearshore profile nourishment. In Proceedings of the 22nd Coastal Engineering Conference, Delft, The Netherlands, 2–6 July 1991; pp. 1998–2009.
22. Hamm, L.; Capobianco, M.; Dette, H.; Lechuga, A.; Spanhoff, R.; Stive, M. A summary of European experience with shore nourishment. *Coast. Eng.* **2002**, *47*, 237–264. [[CrossRef](#)]
23. Martín-Grandes, I.; Hughes, J.; Simmonds, D.J.; Chadwick, A.J.; Reeve, D.E. Novel methodology for one line model calibration using impoundment on mixed beach. In Proceedings of the Coastal Dynamics 2009: Impacts of Human Activities on Dynamic Coastal Processes, Tokyo, Japan, 7–11 September 2009; World Scientific: Singapore, 2009; pp. 1–10.
24. Martín-Grandes, I.; Simmonds, D.J.; Karunaratna, H.; Horrillo-Caraballo, J.M.; Reeve, D.E. Assessing the Variability of Longshore Transport Rate Coefficient on a Mixed Beach. In Proceedings of the Coastal Dynamics, Helsingør, Denmark, 12–16 June 2017; pp. 642–653.
25. Martín-Grandes, I. Understanding Longshore Sediment Transport on a Mixed Beach. Ph.D. Thesis, Plymouth University, Plymouth, UK, 2014.
26. Lamberti, A.; Tomasicchio, G.R. Stone mobility and longshore transport at reshaping breakwaters. *Coast. Eng.* **1997**, *29*, 263–289. [[CrossRef](#)]
27. Tomasicchio, G.R.; D'Alessandro, F.; Frega, F.; Francone, A.; Ligorio, F. Recent improvements for estimation of longshore transport. *Ital. J. Eng. Geol. Environ.* **2018**, *1*, 179–187.
28. Tomasicchio, G.R.; D'Alessandro, F.; Barbaro, G.; Malara, G. General longshore transport model. *Coast. Eng.* **2013**, *71*, 28–36. [[CrossRef](#)]
29. Ahrens, J.P. *Characteristics of Reef Breakwaters, (No. CERC-TR-87-17)*; Coastal Engineering Research Center: Vicksburg, MS, USA, 1987.
30. Van der Meer, J.W. Rock Slopes and Gravel Beaches under Wave Attack. Ph.D. Thesis, Delft Hydraulics Laboratory, Delft, The Netherlands, 1988.
31. Klopman, G.; Stive, M. Extreme waves and wave loading in shallow water. In Proceedings of the Wave and Current Kinematics and Loading: E&P Forum Workshop, Paris, France, 25–26 October 1989.
32. Battjes, J.A.; Groenendijk, H.W. Wave height distributions on shallow foreshores. *Coast. Eng.* **2000**, *40*, 161–182. [[CrossRef](#)]
33. Komar, P.D.; Gaughan, M.K. Airy wave theory and breaker height prediction. In Proceedings of the 13th Conf. on Coastal Engineering, Vancouver, Canada, 29 January 1972; pp. 405–418.
34. Tomasicchio, G.; Lamberti, A.; Guiducci, F. Stone movement on a reshaped profile. In Proceedings of the 24th International Conf. on Coastal Engineering, ASCE, Kobe, Japan, 23–28 October 1994; pp. 1625–1640.

35. Tørum, A.; Sigurdarson, S. PIANC Working Group No. 40: Guidelines for the Design and Construction of Berm Breakwaters. In Proceedings of the Breakwaters, Coastal Structures and Coastlines, London, UK, 26–28 September 2001; pp. 373–384.
36. Pelnard-Considere, R. Essai de theorie de l'evolution des formes de rivage en plages de sable et de galets. In Proceedings of the Les Energies de la Mer: Compte Rendu Des. Quatriemes Journees de L'hydraulique, Paris, France, 13–15 June 1956. rapport 1, 74-1-10.
37. Bruun, P. *Coast. Erosion and the Development of Beach Profiles*; US Beach Erosion Board: Washington, DC, USA, 1954; Volume 44.
38. Dean, R.G. *Equilibrium Beach Profiles: US Atlantic and Gulf Coasts*; Department of Civil Engineering and College of Marine Studies, Newark, University of Delaware: Newark, DE, USA, 1977.
39. Hanson, H.; Kraus, N.C. *GENESIS: Generalized Model. for Simulating Shoreline Change. Report 1. Technical Reference*; Coastal Engineering Research Center: Vicksburg, MS, USA, 1989.
40. Tomasicchio, G.R.; D'Alessandro, F.; Barbaro, G.; Musci, E.; De Giosa, T.M. Longshore transport at shingle beaches: An independent verification of the general model. *Coast. Eng.* **2015**, *104*, 69–75. [[CrossRef](#)]
41. Hanson, H. *GENESIS: A Generalized Shoreline Change Numerical Model for Engineering Use*; Department of Water Resources Engineering, Lund University: Lund, Sweden, 1987.
42. Ozasa, H.; Brampton, A. Mathematical modelling of beaches backed by seawalls. *Coast. Eng.* **1980**, *4*, 47–63. [[CrossRef](#)]
43. Medellín, G.; Torres-Freyermuth, A.; Tomasicchio, G.R.; Francone, A.; Tereszkievicz, P.A.; Lusito, L.; Palemón-Arcos, L.; López, J. Field and numerical study of resistance and resilience on a sea breeze dominated beach in Yucatan (Mexico). *Water* **2018**, *10*, 1806. [[CrossRef](#)]
44. Hamza, W.; Tomasicchio, G.R.; Ligorio, F.; Lusito, L.; Francone, A. A Nourishment Performance Index for Beach Erosion/Accretion at Saadiyat Island in Abu Dhabi. *J. Mar. Sci. Eng.* **2019**, *7*, 173. [[CrossRef](#)]
45. Hallermeier, R.J. Sand transport limits in coastal structure designs. In Proceedings of the Coastal Structures' 83, Washington, DC, USA, 9–11 March 1983; pp. 703–716.
46. Goda, Y.; Takayama, T.; Suzuki, Y. Diffraction Diagrams for Directional Random Waves. In Proceedings of the 16th International Conference on Coastal Engineering, Hamburg, Germany, 27 August–3 September 1978; Volume 1.
47. Larson, M. Numerical modeling. In *Encyclopedia of Coastal Science*; Schwartz, M., Ed.; Springer: Dordrecht, The Netherlands, 2005; pp. 730–733.
48. Bodge, K.R.; Dean, R.G. Short-term impoundment of longshore transport. In Proceedings of the Coastal Sediments, New Orleans, Louisiana, 12–14 May 1987; pp. 468–483.
49. Wang, P.; Kraus, N.C. Longshore sediment transport rate measured by short-term impoundment. *J. Waterw. Port Coast. Ocean Eng.* **1999**, *125*, 118–126. [[CrossRef](#)]
50. Van Wellen, E.; Chadwick, A.; Mason, T. A review and assessment of longshore sediment transport equations for coarse-grained beaches. *Coast. Eng.* **2000**, *40*, 243–275. [[CrossRef](#)]

